Colloid Polym Sci (2002) 280: 725–735
DOI 10.1007/s00396-002-0674-3

ORIGINAL CONTRIBUTION

Kenichi Izawa
Toshiaki Ogasawara
Hideki Masuda
Hirofumi Okabayashi
Michael Monkenbusch
Charmian J. O'Connor

Growth process for fractal polymer aggregates formed by perfluorooctyltriethoxysilane. Time-resolved small-angle X-ray scattering spectra and the application of the unified equation

Received: 28 September 2001
Accepted: 16 January 2002
Published online: 18 April 2002

K. Izawa · T. Ogasawara · H. Masuda
H. Okabayashi (✉)
Department of Applied Chemistry,
Nagoya Institute of Technology,
Gokiso-cho, Showa-ku,
Nagoya 466-8555, Japan
E-mail: fwiw4348@mb.infoweb.ne.jp

M. Monkenbusch
Institut für Festkörperforschung,
IFF Forschungszentrum Jülich,
52425 Jülich, Germany

C.J. O'Connor
Department of Chemistry,
The University of Auckland,
Private Bag 92019, Auckland 1,
New Zealand

Abstract The time-resolved small-angle X-ray scattering (SAXS) profiles, obtained during the polymerization of perfluorooctyltrimethoxysilane catalyzed by different HCl concentrations, have been analyzed using the unified Guinier/power-law equation introduced by Beaucage. SAXS profiles, time-sliced for the reaction mixture catalyzed by dilute HCl, can be perfectly fitted by a simple Beaucage function with only one step of structural hierarchy. The time-resolved SAXS profiles, obtained from the reaction mixtures catalyzed by more concentrated HCl, have led to the conclusion that the growth process of the polymeric aggregate occurs in two steps. This result was successfully explained by application of the unified equation at two structural levels. This conclusion is now corroborated by application of the unified Beaucage equation to evaluation of the growth process of the polymeric precursors.

Introduction

It is well-known that the condensation reaction of alkoxides, such as tetramethylorthosilicate or tetraethoxysilane (TEOS) yields a variety of silicas. Bechtold [1] provided evidence for the existence of polymeric structures in silica solutions. Sakka and Kamiya [2] demonstrated that silica fibers could be pulled from solution. Furthermore, Schaefer and Keefer [3] have examined the fractal characteristics of branched silica polymers by use of small-angle X-ray scattering (SAXS). These studies promoted re-evaluation of the applicability of organic polymer concepts to silica solutions.

Brinker et al. [4] used time-resolved SAXS intensity profiles to follow the development of the reaction in the silicate-forming TEOS/alcohol/water system and the associated sol–gel transition using either an acid or a base catalyst. The results based on the Guinier approximation showed that the size of the silicate cluster in the acid-catalyzed system did not change over time, while for the base-catalyzed system the radius of gyration of the largest aggregates grew linearly during the time in which gelation occurred, i.e. from 20 Å at 1.2 h after the additio n of the base catalyst to 44 Å after 3.8 h.

Keefer [5] discussed the smoothing of the surface of the colloidal particles (fractally rough TEOS clusters) by use of SAXS curves time-resolved on relatively long time scales; however, very little is known about the time-resolved SAXS data within the initial time course (1 h) of the condensation reaction of alkoxide or alkylalkoxide.

The polymeric materials which are produced by condensation of the alkylalkoxysilane molecule [$R\mathrm{Si}(\mathrm{O}\text{–}R')_3$, R = alkyl and R' = methyl or ethyl group] may be regarded as mass-fractal structural materials. When we use the alkylalkoxysilane molecule with long hydrophobic or lipophobic chains for production of the materials, we may assume that self-assembly caused by the hydrophobicity or lipophobicity of the R group occurs in the polymerizing

process [6], providing a local ordering in the polymeric materials which should be reflected in their physical properties. Thus, the alkylalkoxysilane-based polymers can be regarded as organic–inorganic hybrid polymers.

In particular, the silane-coupling agent perfluorooctyltrialkoxysilane is known to furnish hydrophobic and lipophobic properties onto the surface of inorganic materials. A detailed understanding of the condensation process of this silane-coupling agent is very important for practical modification of this surface. With such a practical application in mind, Ogasawara et al. [7] surveyed and analyzed the growth process of fractal perfluorooctyltriethoxysilane (PFOTES) polymers using Guinier's approximation. The principal result was that the growth process of the polymeric precursors occurs in two steps and that the second step may be regarded as a microscopic phase-separation before the onset of the macroscopic phase transition.

In the present study, we present the time-resolved SAXS spectra for the growth process of fractal perfluorooctyltriethoxysilane polymers catalyzed by various HCl concentrations, and we use the unified Guinier/power-law equation [8] to confirm, by curve-fitting, the two-step process for PFOTES–water aggregation.

The unified (Beaucage) equation has been successfully applied to a number of experimental systems [9]. Recently, Stellbrink et al. [10] used small-angle neutrons scattering (SANS) to examine the self-assembly of the styryl–lithium head groups during the early stages of living anionic polymerization. The scattering intensity can be analyzed by the form factor for a mass-fractal structure, as proposed by Beaucage [8] and Beaucage and Schaefer [9].

For data-fitting of SAXS intensity spectra of polymeric mass fractals with arbitrary mass-fractal dimensions, Beaucage [11] described a unified equation in detail, and showed that this unified equation can be substituted for the Debye equation in the random-phase approximation description of polymer blends when the mass-fractal dimension of a polymer coil deviates from 2. In fact, it has been demonstrated that the unified equation can be fitted to describe the SANS and SAXS spectra of various polymers, nonequilibrium growth processes and low-dimensional objects [8]. In particular, such a description of polymeric mass fractals has been successfully applied to the polymerization process which results in the formation of silica-based aerogels [9, 12, 13]. However, very little is known of the application of the unified equation to time-resolved SAXS intensity spectra, which reflect the dynamic growth process in the reaction mixture.

Experimental

Materials

PFOTES was purchased from Fluka Chemical and was used without further purification. The four PFOTES/ethanol/HCl·H_2O (1:1:0.4 weight ratio) systems with different HCl concentrations (0.5, 1.0, 2.0, 3.0 M) were used as the acid-catalyzed reaction mixture at 298 K. Dehydration of ethanol was carried out by use of A-4 molecular sieves.

SAXS measurements

Nine time-resolved SAXS profiles (251 data points covering the range $0.005 < q < 0.21$ Å^{-1}) were measured using a synchrotron radiation X-ray scattering spectrometer (BL-10C) with SAS optics installed at the 2.5 GeV storage ring in the Photon Factory, Tsukuba, Japan. The details of the instruments are given elsewhere [14]. The X-ray wavelength was 1.488 Å, and the sample-to-detector distance was 172 cm. Slit corrections were not carried out because quasi-point-type optics were used. A position-sensitive proportional counter was used for the detection of the X-ray scattering intensity. Fifty-five-second SAXS measurements were repeated after 5-s intervals, using the software SX10CS, immediately before the occurrence of phase separation. One SAXS profile is the summation of SAXS data which were obtained from the measurements repeated five times. The sample solutions were placed in a cell fitted with a pair of mica windows with 1-mm path length and held in a thermostated cell holder maintained at 25.0 ± 0.1 °C by circulating water.

Calibration of the scattering intensity, $I(q)$, was performed using the following equation:

$$I(q) = \frac{I_{\mathrm{sol}}(q)}{C_{\mathrm{sol}} T_{\mathrm{sol}}} - \frac{I_{\mathrm{solv}}(q)}{C_{\mathrm{solv}} T_{\mathrm{solv}}}, \tag{1}$$

where $q = (4\pi/\lambda)\sin\theta$ and $I_{\mathrm{sol}}(q)$, $I_{\mathrm{solv}}(q)$, C_{sol}, C_{solv}, T_{sol}, T_{solv}, 2θ and λ denote the scattering intensities of the solution and pure solvent, the incident X-ray beam intensities for the solution and for the solvent, the X-ray beam transmission through the sample, the scattering angle and the incident wavelength, respectively. Although the T values can be estimated by using the X-ray mass absorption coefficients of the elements in the solution or the solvent, in this present study they were determined as follows. The T_{solv} values were determined from the X-ray beam intensities transmitted through the solvent-filled cell and through a pure lead stearate disk placed just in front of the identical solvent-filled cell. The T_{sol} values were then determined from the beam intensities transmitted through the sample-solution filled cell and through an identical sample solution-filled cell with a lead stearate disk placed in front.

Analysis of the intermediate region of the scattering curve provides information on the detailed structure within a macromolecule. The intermediate region is bounded by the limits $qR_{\mathrm{g}} \gg 1$, $qa \ll 1$, where a is the size of the monomer. In this region, universal power-law behavior, which is independent of both the size of the molecule, R_{g}, and the size of the molecular binding block (monomer), a [15, 16, 17, 18, 19], is predicted, and the simple power law is given by the equation $\log I(q) = \text{constant} + \alpha \log q$, where α is the Porod slope. After considering both the size of the polymeric precursor (R_{g}) and the typical chemical bond distance ($a \approx 3$ Å, for the bonds of the Si–O–Si segment), the region 0.17–0.33 Å^{-1} was defined as the Porod regime [15].

Theoretical background

The Debye equation (Eq. 2) [20, 21] describes well the scattering intensity, $I(q)$, from a polymer chain with a mass fractal of dimension $P = 2$,

$$I(q) = 2G[\mathrm{e}^{-x} - (1 - x)]/x^2, \tag{2}$$

where $x = q^2R_g^2$, and G is a constant. Since it is difficult to describe the scattering function of a polymer system (coil) with a mass-fractal dimension deviating from 2 in terms of simple analytic functions, Eq. (2) is restricted to polymer systems with $P = 2$.

Benoit [22] and Peterlin [23] derived a Debye-like scattering function for arbitrary polymeric mass-fractal scaling in terms of an integral form. They also provided an asymptotic expansion of the integral, yielding the power-law prefactor for arbitrary mass-fractal dimension, which may be compared with the unified Beaucage approach [8].

It is well known that the unified approach (i.e., the unified Guinier exponential/power-law equation) can be extended to describe any number of related structural levels in a material and that two structural levels which exist in a polymer coil can be consistently modeled using this unified equation with only one level of structural hierarchy [11]. In fact, the unified equation has been successfully applied to a number of experimental systems [9, 10].

The unified equation for one structural level is expressed as the summation of two components:

$$I(q) \cong G\exp\left(-q^2R_g^2/3\right) + B(1/q^*)^P, \tag{3}$$

where $q^* = q/[\mathrm{erf}(\mathrm{k}qR_g/6^{1/2})]^3$ in which erf is the error function. G is the Guinier prefactor given by $G = N_p(\rho_e V_p)^2$ (V_p is the volume of a particle and ρ_e is the electron-density difference between the particle and the solvent) and B is a constant prefactor specific to the type of power-law scattering observed, which for arbitrary polymeric-mass fractals can be related to $B = GP/R_g{}^P\Gamma(P/2)$ (polymeric constraint on the unified equation) [8]. P is the mass-fractal dimension of the internal substructure, k is an empirical constant found to be 1.06 and Γ is the Gamma function. The first term in Eq. (3) corresponds to a conventional Guinier approximation which describes the overall properties of the scatterers observed at low q. The second term describes the contributions of scattering arising from the internal substructure, which is resolved in the higher q region. For a diffuse interface $P > 4$ [24], for surface fractals $4 > P > 3$, and for mass fractals $3 > P > 1$.

Extension of Eq. (3) describes the scattering from structures with an arbitrary number, n, of substructural levels. Beaucage and Schaefer [9] developed the following equation (Eq. 4) for two structural levels ($n = 2$).

$$I(q) \cong G\exp\left(-q^2R_g^2/3\right) + B\exp\left(\frac{-q^2R_{sub}^2}{3}\right)\left(\frac{1}{q^*}\right)^P + G_s\exp\left(\frac{-q^2R_s^2}{3}\right) + B_s\left(\frac{1}{q_s^*}\right)^{P_s}, \tag{4}$$

where $q^* = q/\left[\mathrm{erf}\left(qkR_g/6^{1/2}\right)\right]^3$ and $q_s^* = q/\left[\mathrm{erf}\left(qk_sR_s/6^{1/2}\right)\right]^3$. G, B, G_s and B_s are amplitudes. The first term in Eq. (4) describes the large-scale structure of size R_g composed of small-scale structures of size R_s. The second term describes the mass-fractal regime with two structural limits. The final two terms are Eq. (3) for the small substructure with the radius of gyration, R_s. Equation (4) can be used to describe the scattering from a system with multiple-size-scale features.

Under very generally applicable assumptions, Eq. (4) can be extended to describe an arbitrary number of structures using different size scales:

$$I(q) \cong \sum_{i=1}^{n}\left[G_i\exp\left(\frac{-q^2R_{gi}^2}{3}\right) + B_i\exp\left(\frac{-q^2R_{g(i+1)}^2}{3}\right)\left(\frac{1}{q_i^*}\right)^{P_i}\right], \tag{5}$$

where $i = 1$ reflects the largest size structure and $q_i^* = q/\left[erf\left(qk_iR_{gi}/6^{1/2}\right)\right]^3$.

Results

For the polymeric aggregates formed by PFOTES molecules in the reaction mixture, we may assume that the perfluorooctyl chains provide a comparatively large contrast in the electron density between the aggregate and the solvent. This contrast is large compared with that of polymers formed by an alkylalkoxide (e.g., *n*-octyltrimethoxysilane) with a hydrocarbon chain, resulting in the advantage that the SAXS spectra can be measured with a high signal-to-noise ratio on a short time scale. In this sense, PFOTES is especially suitable to study the kinetics of the sol–gel transition process that occurs during the reaction.

Phase behavior of the PFOTES/ethanol/HCl·H_2O system

The time-dependent phase behavior of the PFOTES/ethanol/HCl·H_2O (1:1:0.4 weight ratio) system with different HCl concentrations (0.5, 1.0, 2.0, 3.0 M) was examined by visual inspection (Fig. 1). It was found that the phase behavior of the PFOTES/ethanol/HCl·H_2O system depends not only on the reaction time but also on the concentration of HCl. After mixing PFOTES/ethanol with water/HCl, a transparent one-phase solution was obtained immediately before this phase separation occurred. Subsequently, this transparent solution changed into a two-phase solution (an upper transparent layer and a lower viscous, turbid layer), indicating a phase separation similar to the so-called sol–gel transition.

[A]

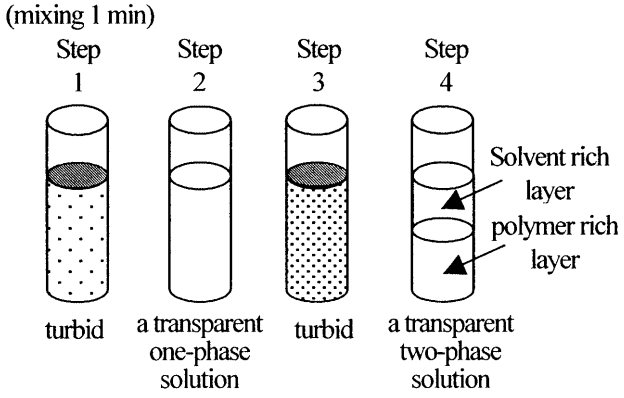

[B]

HCℓ conc.	Step 1	Step 2	Step 3
0.5	ca. 1 min	ca. 240 min	4 – 5 min
1.0	ca. 1 min	ca. 120 min	1 – 2 min
2.0	ca. 1 min	ca. 50 min	1 – 2 min
3.0	ca. 1 min	ca. 40 min	1 – 2 min

Fig. 1. Phase behavior of the perfluorooctyltriethoxysilane (*PFOTES*)/ethanol/HCl·H_2O system

The PFOTES/ethanol/HCl·H_2O system stayed in a transparent one-phase solution for about 240 min, then it became turbid for 4–5 min before the phase separation finally occurred. For the sample system with 2.0 M HCl, the time interval for the transparent solution was 75 min and the turbid state lasted for 1–2 min. From visual inspection of these reaction mixtures, we found that an increase in the HCl concentration reduces the time delay for the onset of the macroscopic sol–gel-like transition.

We have confirmed from proton NMR spectra (not shown) that the upper transparent layer and the lower transparent and viscous layer are solvent-rich and polymer-rich, respectively [7].

Time-resolved SAXS spectra of the PFOTES/ethanol/HCl·H_2O systems

Representative time-resolved SAXS profiles for the 0.5 and 2.0 M HCl-catalyzed systems are shown in Fig. 2. The SAXS profiles strongly depend on the reaction time and the HCl concentration, reflecting the growth process of the polymeric aggregates in the reaction mixtures. In the initial stage of the reaction, the profile is characteristic of a fractal polymer aggregate. However, the intensity of each profile in the lower q range increases with time, until finally the profile comes close to that characteristic of silicate polymers [25], indicating that it is the reaction processes which result in the sol–gel-like transition.

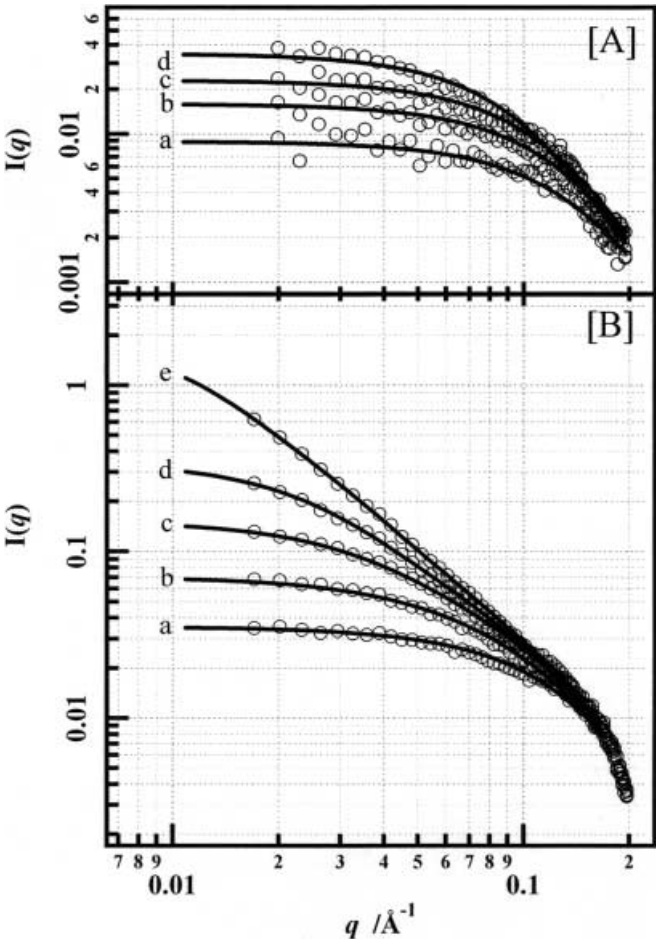

Fig. 2. Time-resolved small-angle X-ray scattering (SAXS) profiles: **A** 0.5 M (*a*) 1,320 s, (*b*) 2,640 s, (*c*) 3,980 s, (*d*) 6,640 s and **B** 2.0 M (*a*) 870 s, (*b*) 1,830 s, (*c*) 2,770 s, (*d*) 3,700 s, (*e*) 4,620 s) HCl-catalyzed systems and *solid curves* fitted by Eqs. (3) (for the 0.5 M HCl system) and (4) (for the 2.0 M HCl system)

The Guinier law [$I(q) = I(0)\exp(-q^2R_g^2/3)$, where $I(0)$ is the zero-angle scattering intensity and R_g is the radius of gyration], was applied to the time-resolved SAXS curves in the region $0.034 < q < 0.06$ Å^{-1} in order to examine the HCl-concentration dependence of the kinetics for the growth process of the polymeric precursors. The time dependence of the radius of gyration of the largest polymeric precursors which were obtained by Guinier plots [$\ln I(q)$ versus q^2, $q \approx 8.53\times10^{-3}$–$4.82\times10^{-2}$, Fig. 3A], is shown in Fig. 3B and the R_g values are listed in Table 1. For the sample systems with HCl concentrations of 1.0, 2.0 and 3.0 M, we find that growth of the polymeric precursors occurs in a two-step process, on a short time scale, immediately prior to phase separation. An increase in the HCl concentration evidently speeds up the time for commencement of the growth process for the second step. This commencement time may be regarded as a transition during which microstructural variation occurs before the onset of the macroscopic

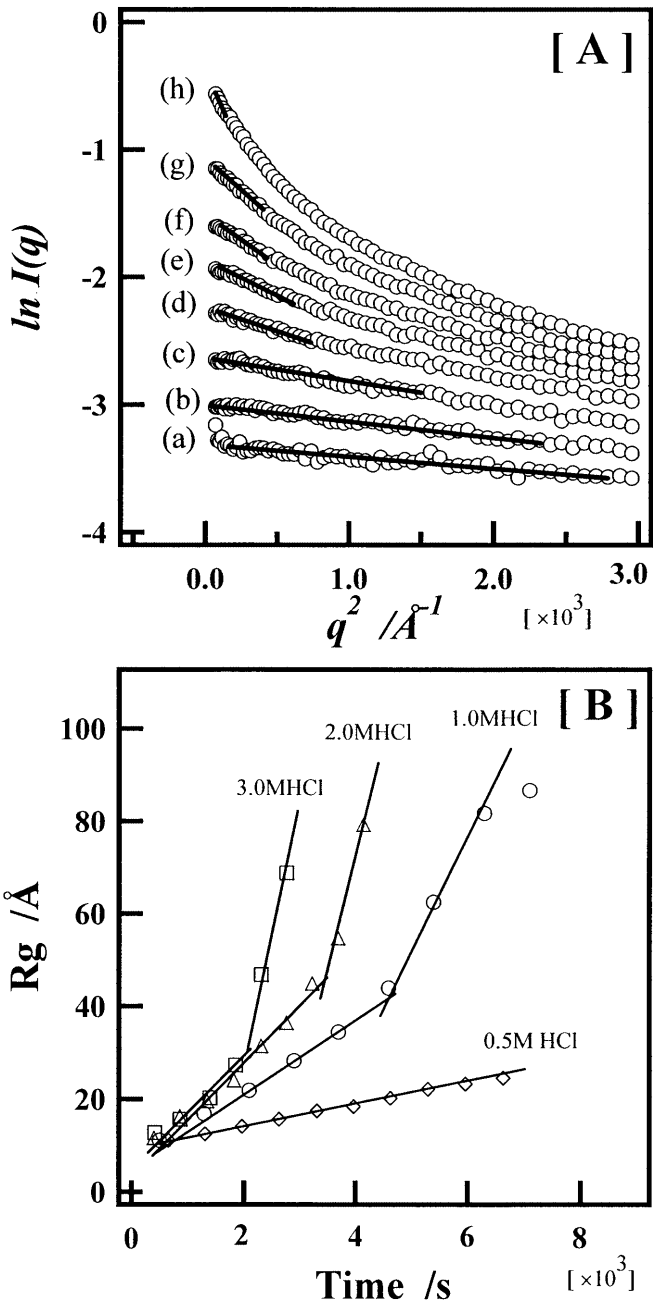

Fig. 3. **A** Guinier plots for the 2.0 M HCl-catalyzed PFOTES/ethanol system: (*a*) 870 s (*q* region: 0.012–0.052 Å^{-1}), (*b*) 1,350 s (*q* region: 0.008–0.048 Å^{-1}), (*c*) 1,830 s (*q* region: 0.007–0.040 Å^{-1}), (*d*) 2,320 s (*q* region: 0.007–0.027 Å^{-1}), (*e*) 2,770 s (*q* region: 0.009–0.026 Å^{-1}), (*f*) 3240 s (*q* region: 0.009–0.020 Å^{-1}), (*g*) 3,700 s (*q* region: 0.009–0.022 Å^{-1}), (*h*) 4,150 s (*q* region: 0.008–0.012 Å^{-1}) and **B** radius of gyration (Guinier R_g) versus time for 0.5 M (*diamonds*), 1.0 M (*circles*), 2.0 M (*triangles*) and 3.0 M (*squares*) HCl-catalyzed systems

sol–gel transition. Furthermore, an increase in the HCl concentration increases the slope of the linear R_g versus t relationship, indicating that high acidity promotes the growth of the polymeric precursors.

For the 0.5 M HCl-catalyzed system, it seems that the growth of the small precursors is very slow and the commencement time for the second step may be later than the time range measured in this present study, probably caused by the very small size of the reactive clusters generated in the reaction mixture.

The time-resolved SAXS curves measured for the four PFOTES/ethanol/HCl·H_2O systems were analyzed by use of a power law. The values of the dimension (P) thus obtained are listed in Table 1. The separated spectra of the 2.0 M HCl-catalyzed system showing slopes of the Porod region are shown in Fig. 4. The P value strongly depends upon the reaction time and the HCl concentration, indicating that the growth of the microstructure of the PFOTES polymeric aggregates depends on the time and the HCl concentration.

For the 0.5 and 1.0 M HCl-catalyzed systems during the early initial stage it is found that the P values in the range $2 < P < 3$ are characteristic for mass fractals; however, the 2.0 and 3.0 M HCl-catalyzed systems exhibit values of $P = 5.0$–5.5 as expected for scattering from a particle with a diffuse interface.

In the SAXS profiles of the 0.5 M HCl-catalyzed system (Fig. 4A), weak maxima seem to appear at $q \approx 0.034$–0.035 Å^{-1}, and, as the reaction proceeds, the intensities become very weak until finally they disappear. This observation may be explained as follows. In the initial growth process, the formation of colloidally unstable nuclei and coagulation of nuclei probably occurs, resulting in an increase in size but a decrease in number as the particles are stabilized.

Application of the unified equation

The time dependent SAXS intensity patterns from the reaction mixtures catalyzed by 0.5 and 2.0 M HCl were analyzed by use of the unified equations (Eqs. 3, 4) as follows.

In order to reduce the number of free parameters (G, B, R_g and P) to three, the assumption of a "polymeric constraint" was made, and then the unified equation (Eq. 3) at one structural level was first fitted to the observed scattering data in the region $0.04 < q < 0.21$ Å^{-1}. In particular, for fitting of the SAXS data of the 2.0 M HCl-catalyzed system, the R_g and P values, which were obtained from the analyses based on one structural level in the low- and high-q regions, were set equal to the same G_s, R_s and P_s as pertained to the initial values in Eq. (4) and provided $R_{sub} = R_s$.

Analysis at one structural level

We fitted the unified equation (Eq. 3), instead of the Guinier approximation to the time-resolved SAXS

Table 1. R_g (Guinier approximation) and P (power-law) values for the 0.5, 1.0, 2.0 and 3.0 M HCl-catalyzed systems

0.5 M HCl			1.0 M HCl			2.0 M HCl			3.0 M HCl		
Time (s)	R_g (Å)	P	Time (s)	R_g (Å)	P	Time (s)	R_g (Å)	P	Time (s)	R_g (Å)	P
670	11.0	2.64	500	11.1	2.64	410	11.5	4.27	410	12.8	4.86
1,320	12.5	2.78	1,300	16.8	2.78	870	16.2	4.58	870	15.7	5.05
1,980	14.1	2.80	2,100	21.8	2.80	1,350	19.4	5.09	1,400	20.3	5.18
2,640	15.6	2.80	2,900	28.2	2.80	1,830	23.9	5.13	1,860	27.4	5.31
3,980	18.7	2.94	3,700	34.4	2.82	2,320	31.3	5.15	2,310	46.8	5.40
4,640	20.1	2.93	4,600	43.9	2.94	2,770	36.3	5.17	2,770	68.8	5.51
5,300	22.0	2.94	5,400	62.4	2.93	3,240	44.8	5.19			
5,970	23.2	2.99	6,300	81.7	2.94	3,700	54.1	5.11			
7,300	24.6	2.98	7,100	86.6	2.99	4,620	79.1	5.12			

curves in the region $0.04 < q < 0.21$ Å^{-1} for the two PFOTES/ethanol systems catalyzed by 0.5 M HCl. The R_g values obtained using the Guinier approximation and the P values obtained by use of a power law were used as the initial values of R_g and P in Eq. (3). All the SAXS intensity data in this region for the 0.5 M HCl-catalyzed system were perfectly fitted by Eq. (3). The best fits to the data observed for these reaction mixture systems are shown as solid lines in Fig. 2A. The calculated parameters (G, R_g, P) are listed in Table 2 together with their corresponding errors. The time dependence of the calculated R_g value is also shown in Fig. 5A, together with that of the Guinier R_g value. It is found that the R_g value increases with an increase in reaction time in the range 13–19 Å and that the dimensions of the mass fractals become approximately constant in the range 2.83–2.92.

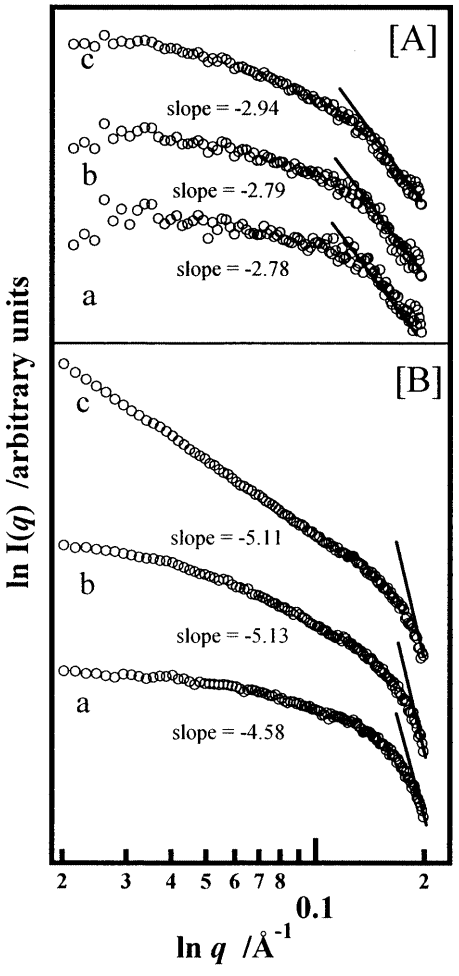

Fig. 4. Separated time-resolved SAXS spectra for **A** the 0.5 M ((*a*) 1,320 s, (*b*) 2,640 s, (*c*) 5,300 s) and **B** for the 2.0 M ((*a*) 870 s, (*b*) 2,320 s, (*c*) 5,110 s) HCl-catalyzed systems showing slopes of the Porod region

Analysis at two structural levels

The unified equation (Eq. 3) was applied to try and describe the time-resolved SAXS profiles for the 2.0 M HCl-catalyzed reaction mixture. However, the whole profiles in the 0.04–0.21-Å^{-1} region could not be described on the basis of one structural level.

Based on the assumption of a polymeric constraint [8], we fitted Eq. (4) at two structural levels to the observed SAXS curves of the 2.0 M HCl-catalyzed system, leading to good agreement between the observed and calculated intensity data (Fig. 2B). The extracted parameters are listed in Table 3.

For the 2.0 M HCl reaction system, the calculated R_g values are plotted as a function of reaction time in Fig. 5B. The time dependence of the calculated R_g values is in good agreement with the results obtained from the Guinier approximation within a reaction time of 4,140 s, but not with the two Guinier radius (R_g') obtained for reaction times greater than 4,600 s. This disagreement may be due to the nature of the R_g' values, which cannot be used to discuss the growth process since they come from the condition $R_g^2 q^2 < 1$ in the Guinier approximation (in fact, $R_g' = 122$ and 165 Å for 4,620 and 5,110 s, respectively, providing values of $R_g'^2 q^2 = 2.0$ and 3.2, respectively, which deviate greatly from unity). In order to obtain the true Guinier R_g values for reaction times immediately before phase separation, we need to measure the SAXS data in the smaller-angle region,

Table 2. The parameters calculated using Eq. (3) with the best fit for the 0.5 M HCl-catalyzed system. The residual was calculated as residual = $\sum\{[I(q_i) - I(q_i)^*]/\sqrt{I(q_i)}\cdot\sqrt{I(q_i)}\}^2$, where $I(q_i)$ is observed and $I(q_i)^*$ is calculated using Eq. (3)

Time (s)	B ($\times 10^{-5}$)	G ($\times 10^{-2}$)	R_g	P	Residual ($\times 10^{-5}$)
670	0.70	0.39	13.0	2.83	0.15
1,320	2.48	0.89	13.0	2.63	0.12
1,980	1.83	1.17	14.3	2.77	0.10
2,640	2.01	1.59	14.2	2.86	5.74
3,320	2.30	2.30	15.2	2.81	5.26
3,980	2.23	2.30	15.8	2.85	5.35
4,640	1.84	3.14	16.8	2.87	5.96
5,300	2.78	3.14	17.0	2.80	7.19
5,970	1.97	3.05	18.0	2.87	7.41
6,640	1.68	3.49	19.0	2.92	9.09

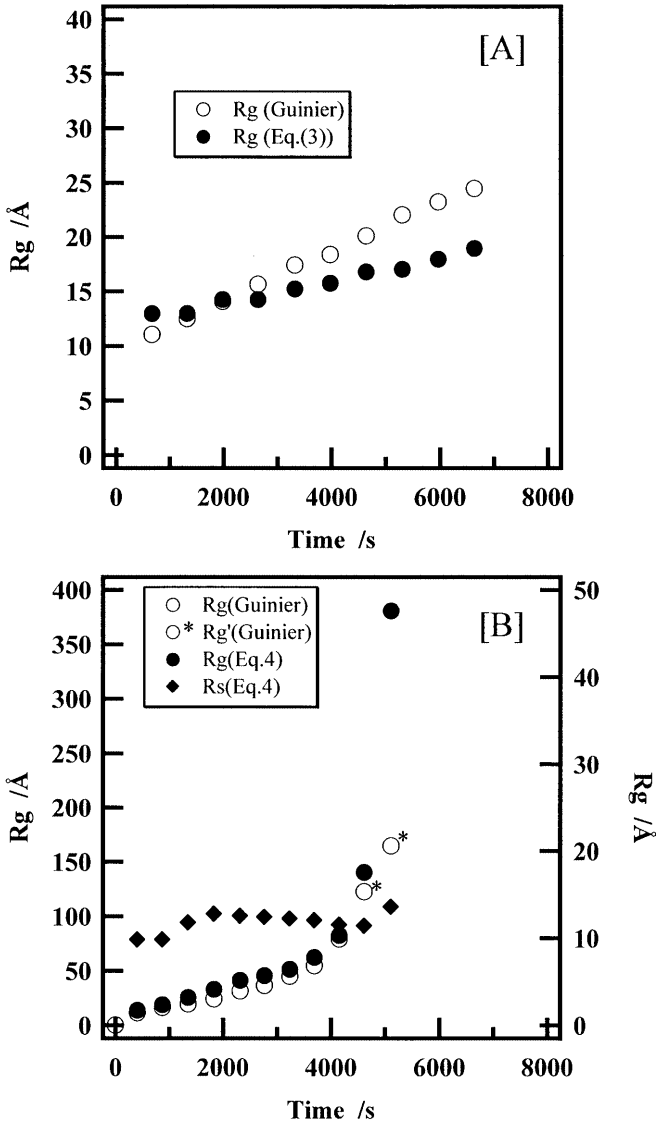

Fig. 5. **A**]R_g values (Guinier approximation) for the 0.5 M HCl-catalyzed system and R_g values calculated using Eq. (3) and **B**]R_g values (Guinier approximation) for the 2.0 M HCl-catalyzed system and R_g and R_s values calculated using Eq. (4) [○*: R_g values (R_g') at 4,620 and 5,110 s are 122 and 165 Å, respectively]

although, unfortunately, this was not possible with the present instrument. However, a marked variation in the slope between the two approximately linear regimes of $R_g(t)$ versus t reveals that the growth of polymeric aggregates proceeds in two steps. That is, the formation of small clusters ($R_s = 10$–14 Å) predominantly occurs in the initial step, while in the second step, clusters with a larger size ($R_g = 14$–380 Å) are formed and their growth proceeds rapidly.

The unified equation was also fitted to the time-resolved SAXS data of the 3.0 M HCl-catalyzed system. The results, which provided good agreement between the observed and calculated intensity data, also reveal that the two-step process exists during the growth of polymeric aggregates. The extracted parameters are listed in Table 4 (observed and calculated spectra not shown).

From the parameters P and P_s, extracted from the calculations for the 2.0 and 3.0 M HCl-catalyzed systems, the P value of polymeric precursors with large size is very close to unity at the beginning of the reaction; however, it increases with an increase in reaction time until finally it becomes close to 2 immediately before the occurrence of phase separation. In particular, the P_s value of 3.10 obtained from the scattering data in the initial stage is close to the dimension for the mass fractal, and the reaction progress brings about the P_s value of 4.75–6.55 for a compact particle with a diffuse interface.

Discussion

The kinetic model, which explains the growth processes of polymerization and aggregation that occur far from equilibrium, has been presented by Witten et al. [26], Sander [27], Schaefer [28] and Daoud et al. [29] for the growth process of silica polymers. Schaefer [28] described the kinetic model of monomer–cluster (MC) growth and cluster–cluster (CC) growth. The MC and CC growth models may be modified to conform to the growth process of the PFOTES polymeric precursors. The mechanism for the growth process of the PFOTES

Table 3. The parameters calculated using Eq. (4) with the best fit for the 2.0 M HCl-catalyzed system. The residual was calculated as residual $= \sum \left\{ [I(q_i) - I(q_i)^*] / \sqrt{I(q_i)} \right\}^2$, where $I(q_i)$ is observed and $I(q_i)^*$ is calculated using Eq. (4)

Time (s)	B ($\times 10^{-4}$)	G	R_g	P	B_s ($\times 10^{-8}$)	G_s ($\times 10^{-2}$)	R_s	P_s	Residual ($\times 10^{-5}$)
410	0.19	0.02	13.2	1.09	0.02	0.18	9.89	3.41	3.44
870	8.81	0.03	20.6	1.30	0.02	1.05	9.75	4.59	3.82
1,350	3.33	0.02	27.2	1.54	0.33	2.06	11.4	5.42	4.45
1,830	3.10	0.05	34.3	1.62	0.23	2.33	11.8	5.58	3.92
2,320	2.82	0.08	41.4	1.68	8.08	2.86	12.6	6.04	3.41
2,770	3.02	0.12	45.5	1.75	5.71	2.66	12.3	6.24	3.25
3,240	2.72	0.19	51.4	1.83	7.03	2.43	12.2	6.13	3.88
3,700	2.71	0.32	62.8	1.87	5.31	2.41	12.2	6.27	3.77
4,140	2.69	0.64	84.3	1.90	4.92	2.52	12.4	6.28	5.56
4,620	2.33	2.02	137	1.98	4.50	2.70	12.4	6.28	5.74
5,110	2.14	13.0	380	1.97	4.08	3.86	13.6	6.31	4.69

Table 4. The parameters calculated using Eq. (4) with the best fit for the 3.0 M HCl-catalyzed system. The residual was calculated as residual $= \sum \left\{ [I(q_i) - I(q_i)^*] / \sqrt{I(q_i)} \right\}^2$, where $I(q_i)$ is observed and $I(q_i)^*$ is calculated using Eq. (4)

Time (s)	B ($\times 10^{-4}$)	G	R_g	P	B_s ($\times 10^{-8}$)	G_s ($\times 10^{-2}$)	R_s	P_s	Residual ($\times 10^{-5}$)
410	0.02	0.02	15.2	1.12	0.02	0.03	7.36	3.10	4.97
870	1.22	0.01	41.4	1.30	0.01	2.96	12.3	4.75	4.10
1,400	1.83	0.03	43.4	1.46	0.20	3.35	12.6	5.65	3.52
1,860	2.84	0.05	41.8	1.56	0.10	3.33	12.7	5.97	3.59
2,310	3.16	0.09	42.5	1.66	4.63	3.04	12.5	6.38	3.60
2,770	3.69	0.15	47.4	1.72	3.68	3.13	12.4	6.55	3.78

polymeric precursors, which was presented previously [7], can be summarized as follows.

In the initial stage, we may conclude that the growth of monomers to form small clusters (i.e., MC growth) is predominant, on the basis of the time-resolved ^{1}H NMR spectral evidence [7] that the population of reactive monomers is high compared with that in the second step. In the second stage, further growth of small clusters (i.e., CC growth) arising from a condensation reaction between small clusters predominantly continues until finally the macroscopic sol–gel transition occurs.

The mechanism of CC growth in the second stage is important in connection with the mechanism of the sol–gel transition. The idea that polymeric structures exist, which are weakly cross-linked with each other in the earlier reaction stage of the TEOS/alcohol system, as proposed by Brinker et al. [4], may be applied to the growth process of the PFOTES polymeric precursors in the second stage. Relatively small clusters of the PFOTES precursors will probably be initially only weakly cross-linked with each other. However, extensive cross-linking will proceed and the extent of cross-linking will become greater, until finally macroscopic phase separation into a solvent-rich upper layer and a polymer-rich lower layer occurs.

We emphasize that a PFOTES molecule has a bulky perfluorooctyl chain with both hydrophobic and lipophobic properties. Accordingly, the effect of the hydrophobicity and lipophobicity of this bulky chain, in addition to the cross-linking effect, must be considered for the growth process of the PFOTES polymeric precursors. That is, during the growth process, both hydrophobic and lipophobic interactions probably exist between the clusters containing perfluorooctyl chains. Such interactions result in the formation of giant aggregates through self-assembly of the polymeric precursors or clusters with both hydrophobic and lipophobic properties.

The values of R_g of 11–25 Å of the polymeric precursors formed in the reaction mixtures of the 0.5 M HCl-catalyzed system probably imply the existence of small aggregates with a mass-fractal structure ($P = 2.6$–3.0) (Table 1), which involves self-assembled perfluorooctyl moieties in the microstructure.

The scattering intensities from the samples were not described in absolute intensity units, since the scattering intensity $I(0)$ from the standard was not measured in this study. Accordingly, it is difficult to extract valid aggregation numbers of an aggregate. Therefore, a tentative approach was made to obtain the aggregation numbers as follows.

For the 0.5 M HCl-catalyzed system, the intercepts of the two lines [R_g (Guinier approximation) versus t plot] and [R_g (calculated by the unified equation (Eq. 3) versus t plot] in the initial step yield the R_g values at $t = 0$: $R_g = 9.75$ Å for the Guinier approximation and

$R_g = 11.36$ Å for the calculation by the unified equation. If we consider a monomeric PFOTES molecule as a rod with a volume of 860.7 Å^3, we can estimate the aggregation number, n, of the PFOTES aggregates at $t = 0$ as n≅[the volume of a sphere with R_g $(t = 0)$]/860.7 Å^3. Thus, values of $n = 4.5$ (Guinier approximation) and $n = 7.1$ (unified equation Eq. 3 calculation) were obtained, implying that the PFOTES molecules form small aggregates with aggregation number of 5–7 at zero reaction time, their size probably being a consequence of the hydrophobicity and lipophobicity of the perfluorooctyl chain.

We confirmed by time-resolved gel-permeation chromatography profiles that a relatively large number of PFOTES molecules remain unhydrolyzed in the reaction mixture of the 0.5 M HCl-catalyzed system. Furthermore, since a PFOTES molecule easily forms the solvated-type complex $[R_1Si(OEt)_3(OHEt)_{m-3}]$ in ethanol [30], the PFOTES molecules in the ethanol solution may be in a complex state.

Thus, we may assume that the small aggregates which contain the unhydrolyzed PFOTES monomers and the solvated-type complex are predominant in the PFOTES/ethanol system catalyzed by low HCl concentration. Accordingly, the network structure of Si–O–Si bonds may be scarce in this type of aggregate. That is, this kind of aggregate probably does not contain an internal fine silica gel like core structure (Fig. 6A). In this case, the rapid growth of an aggregate probably does not occur, i.e., accretion is slow.

The Guinier R_g values, 80–90 Å, of the largest polymeric aggregates for the 1.0 M HCl-catalyzed system (Table 1) which exist immediately prior to the macroscopic phase separation probably imply the existence of giant aggregates with a mass-fractal structure ($P = 2.6$–3.0). For the 2.0 M HCl system, it may be assumed that giant aggregates exist with Guinier $R_g \approx 80$ Å. However, considering the P values (5.0–5.3) for this reaction system, the aggregate may involve diffuse interfaces. The reason is discussed later.

Thus, the HCl-concentration dependence of the Guinier R_g value which was obtained from the present SAXS data provides the "two-step model" for the growth process of the polymeric precursors to large-scale self-assembled aggregates as described earlier.

In the PFOTES/ethanol reaction mixtures catalyzed by different HCl concentrations, we may expect a marked variation of the morphology of polymeric aggregates to occur in the growth process. The unified equation is a good approximation for the description of such a morphological variation depending upon the reaction time.

In particular, the unified equation (Eq. 3) successfully describes the whole SAXS data in the $0.018 < q < 0.196$ Å^{-1} region time-resolved for the 0.5 M HCl-catalyzed PFOTES reaction system, since the

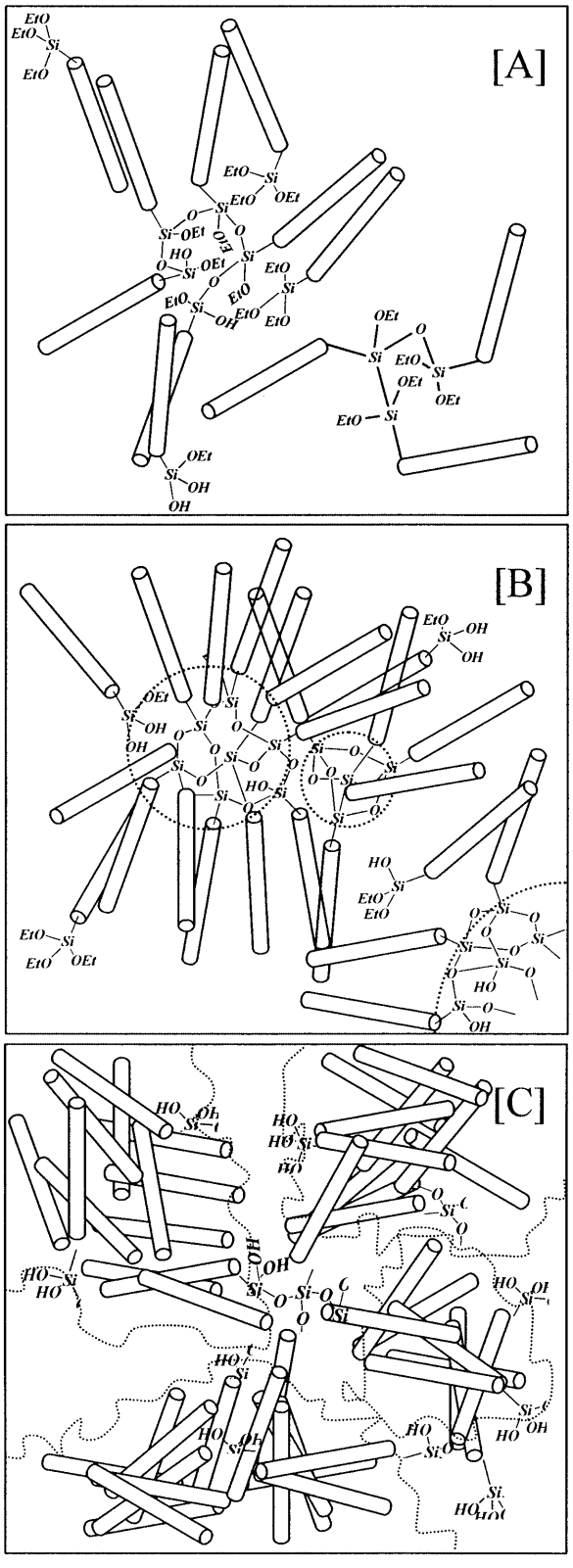

Fig. 6. Schematic models of small aggregates **A** without the core and **B** with the core and **C** of larger aggregates

aggregates with smaller size are predominant in this reaction mixture and the time-dependence of the size is not marked. However, Eq. (3) on one structural level does not describe the whole SAXS data in the $0.018 < q < 0.196$ Å^{-1} region for the reaction mixtures catalyzed by higher HCl concentrations (2.0 and 3.0 M HCl). This fact indicates that the growth of polymeric aggregates for the high-HCl-concentration systems rapidly occurs in two steps and that large polymeric aggregates as well as smaller aggregates are also formed in the reaction mixtures. We found that the unified equation (Eq. 4), at two structural levels, successfully describes the SAXS data of the reactions catalyzed by the presence of higher HCl concentrations.

Thus, the use of the unified equation (Eq. 4) makes it possible to evaluate the variation in the size and morphology of polymeric aggregates with two different sizes (i.e., small and large aggregates) in the reaction process, as seen in Tables 3 and 4.

For the 2.0 and 3.0 M HCl systems, the calculated R_g value of the large aggregates rapidly increases in a two-step process with reaction time (Tables 3, 4). This tendency is in good agreement with that of the time dependence for the Guinier R_g values (Fig. 5B). However, the calculated R_s value of the small aggregates converges on the constant values (13–14 Å), although it increases in the initial stage. It is evident that the constant R_s values are relatively small compared with the R_g value calculated by applying Eq. (3) to the 0.5 M HCl system (which has no tendency to converge). This result may indicate that the size of small aggregates formed under high HCl concentration is limited.

It is very interesting to compare the P_s and P values calculated by using Eq. (4). For the 2.0 and 3.0 M HCl systems, the P_s value of the small aggregates changes from 3.10 to 6.31 (or 6.55) with time, implying that the morphology of the small aggregates formed under conditions of high acidity varies from surface fractal to particles with diffuse interface. However, the value of the mass-fractal dimension of the large aggregates changes from 1.12 to 1.97 (or 1.72) with reaction time. Such a variation of the P throughout the reaction should be regarded as a structural transition.

The mechanism for the formation of particles with a diffuse interface may be explained as follows. When the concentration of HCl is high, most of the ethoxy groups of the PFOTES molecules are probably hydrolyzed, and, as a consequence, the condensation reaction between the silanol (SiOH) groups occurs, bringing about a particle with a Si–O–Si bonding network structure inside. As the reaction proceeds, the network structure expands to become the core of a particle with the perfluorooctyl chains on the outside (Fig. 6B). We may assume that in this particle the diffuse interface exists between the core and the perfluorooctyl chains, leading to the dimension $P > 4$.

In general, the silicic acid monomer, $Si(OH)_4$, has a strong tendency to polymerize in such a way that in the polymer there is a maximum of siloxane (Si–O–Si) bonds and a minimum of uncondensed SiOH groups [31]. Thus, in the earliest process of polymerization, the condensation reaction quickly leads to ring structures (e.g., the cyclic tetramer), which condense internally to the compact state with the SiOH groups remaining on the outside. This concept may be modified to conform to the growth process of the PFOTES polymeric aggregates when the concentration of HCl is high.

For the case of the hydrolyzed PFOTES molecule $[CF_3(CF_2)_5CH_2–CH_2–Si(OH)_3]$, bulky, rigid and rodlike perfluorooctyl chains probably hinder the three-dimensional growth of the siloxane bond network. This steric hindrance may induce the formation of cyclic structures, which are limited in size and which promote the formation of a spherical particle with the shell portion consisting of perfluorooctyl chains and a siloxane bond core. Such a small particle with a tight core and the dense perfluorooctyl chains may grow very slowly, since the silanol (SiOH) groups which remain unreacted are probably isolated or incorporated into the core (Fig. 6B).

However, in addition to the cyclic structures, small fractal structures (so-called lattice animals [32]), which are randomly branched analogs of self-avoiding linear chains, may be present in the initial stage of the reaction (Fig. 6C). Those small mass-fractal precursors may serve as seeds for the formation of giant mass-fractal polymeric aggregates with dimension $P = 1–2$. This growth process may be reflected in the variation of R_g and P values extracted from the results using Eq. (4) (Tables 3, 4). Since a bulky and rigid perfluorooctyl chain can be regarded as a rod, we may consider that these small aggregates (e.g., dimers or trimers), which will be formed at the beginning of the reaction, to be rodlike, leading to a mass-fractal dimension close to unity. However, the growth of small rodlike aggregates to giant aggregates may bring about the transition from $P \approx 1$ to $P \approx 2$.

Conclusions

The time-resolved SAXS intensity spectra measured during the polymerization of PFOTES catalyzed by different HCl concentrations were analyzed using unified equations at one and two structural levels. The unified equations at one structural level were perfectly fitted to the SAXS data obtained from the reaction mixture catalyzed by low HCl concentration, reflecting the existence of small aggregates. The SAXS spectra of the reaction mixtures catalyzed by high (2.0 and 3.0 M) HCl concentrations were successfully described by the unified equation at two structural levels, providing the result

that the growth process occurs in the two steps. The unified equation successfully describes the growth process of polymeric aggregates. Furthermore, by using the extracted parameters we successfully explained the variation in the size and the morphology of aggregates formed in the reaction mixtures.

References

1. Bechtold MF (1955) J Phys Chem 59:532
2. Sakka S, Kamiya K (1982) J Non-Cryst Solids 48:31
3. Schaefer DW, Keefer KD (1984) Phys Rev Lett 53:1383
4. Brinker CJ, Keefer KD, Schaefer DW, Ashley CS (1982) J Non-Cryst Solids 48:47
5. Keefer KD (1984) Mater Res Soc Symp Proc 32:15
6. Jönsson B, Lindman B, Holmberg K, Kronberg B (1998) Surfactants and polymers in aqueous solution. Wiley, Chichester, p 31
7. Ogasawara T, Izawa K, Hattori N, Okabayashi H, O'Connor CJ (2000) Colloid Polym Sci 278:293
8. Beaucage G (1996) J Appl Crystallogr 29:134
9. Beaucage G, Schaefer DW (1994) J Non-Cryst Solids 172–174:797
10. Stellbrink J, Willner L, Jucknischke O, Richter D, Lindner P, Fetters LJ, Huan JS (1998) Macromolecules 31:4189
11. Beaucage G (1995) J Appl Crystallogr 28:717
12. Beaucage G, Ulibarri TA, Black E, Schaefer DW (1995) In: Mark JE, Lee CY, Bianconi PA (eds) Organic hybrid materials. ACS symposium series 585. American Chemical Society, Washington, DC, p 97
13. Hua DW, Anderson J, Hareid S, Smith DM, Beaucage G (1994) In: Cheetham AK, Brinker CJ, Mecartney ML, Sanchez C (eds) Better ceramics through chemistry 6. Materials Research Society Proceedings vol 346. Materials Research Society, Pittsburgh, Pa, p 985
14. Ueki T, Hiragi Y, Kataoka M, Inoko Y, Amemiya Y, Izumi Y, Tagawa H, Muroga Y (1985) Biophys Chem 23:15
15. Porod G (1951) Kolloid Z 124:83
16. Daoud M, Joanny JF (1981) J Phys (Paris) 42:1359
17. Witten TA, Sander LM (1981) Phys Rev Lett 47:1400
18. Meakin P (1983) Phys Rev Lett 51:1119
19. Schaefer DW, Keefer KD, Aubert JH, Rand PB (1986) In: Hench LL, Ulrich DR (eds) Science of ceramic chemical processing. Wiley, New York, p 140
20. Debye P (1947) J Phys Colloid Chem 51:18
21. Debye P (1945) Tech Rep 637 to Rubber Reserve Co, reprinted in Debye P (1954) The collected papers of Peter JW Debye. Interscience, New York
22. Benoit H (1957) Compt Rend 245:2244
23. Peterlin A (1953) Makromol Chem 9:244
24. Korberstein JT, Morra B, Stein RS (1980) J Appl Crystallogr 13:34
25. Keefer KD, Schaefer DW (1986) Phys Rev Lett 56:2376
26. Witten TA, Cates ME (1986) Science 232:1607
27. Sander LM (1987) Sci Am 256:94
28. Schaefer DW (1989) Science 243:1023
29. Daoud M, Martin JE (1989) In: Avenir D (ed) The fractal approach to heterogeneous chemistry. Wiley, New York, pp 109–130
30. Einaga H (2000) Inorganic synthesis in solution as a reaction field. Baifukan, Tokyo, p 169
31. Iler RK (1979) The chemistry of silica – Solubility, polymerization, colloid and surface properties and biochemistry. Wiley, New York, p 175
32. Daoud M, Family F (1984) J Phys Lett 45:L151